BIOCHEMISTRY
including biophysical chemistry & molecular biology

Article

pubs.acs.org/biochemistry

Initial O_2 Insertion Step of the Tryptophan Dioxygenase Reaction Proposed by a Heme-Modification Study

Ryu Makino,*[,†] Eiji Obayashi,[‡] Hiroshi Hori,[§] Tetsutaro Iizuka,[∥] Keisuke Mashima,[†] Yoshitsugu Shiro,*[,∥] and Yuzuru Ishimura[⊥]

[†]Department of Life Science, College of Science, Rikkyo University, Nishi-ikebukuro 3-34-1, Toshima-ku, Tokyo 171-8501, Japan
[‡]Department of Biochemistry, Shimane University School of Medicine, Izumo, Shimane 693-8501, Japan
[§]Center for Quantum Science and Technology under Extreme Conditions, Osaka University, Toyonaka, Osaka 560-8531, Japan
[∥]RIKEN Harima Institute/Spring 8, 1-1-1 Kouto, Mikazuki-cho, Sayo-gun, Hyogo 679-5148, Japan
[⊥]Department of Biochemistry, School of Medicine, Keio University, 35 Shinanomachi, Shinjuku-ku, Tokyo 160-8582, Japan

Supporting Information

ABSTRACT: L-Tryptophan 2,3-dioxygenase (TDO) is a protoheme-containing enzyme that catalyzes the production of *N*-formylkynurenine by inserting O_2 into the pyrrole ring of L-tryptophan. Although a ferrous−oxy form (Fe^{2+}−O_2) has been established to be an obligate intermediate in the reaction, details of the ring opening reaction remain elusive. In this study, the O_2 insertion reaction catalyzed by *Pseudomonas* TDO (PaTDO) was examined using a heme-modification approach, which allowed us to draw a quantitative correlation between the inductive electronic effects of the heme substituents and the substituent-induced changes in the functional behaviors of the ferrous−oxy form. We succeeded in preparing reconstituted PaTDO with synthetic hemes, which were different with respect to the inductive electron-withdrawing nature of the heme substituents at positions 2 and 4. An increase in the electron-withdrawing power of the heme substituents elevated the redox potential of reconstituted PaTDO, showing that the stronger the electron-withdrawing ability of the heme substituents, the lower the electron density on the heme iron. The decrease in the electron density of the heme iron resulted in a higher frequency shift of the C−O stretch of the heme-bound CO and enhanced the dissociation of O_2 from the ferrous−oxy intermediate. This result was interpreted as being due to weaker π back-donation from the heme iron to the bound CO or O_2. More importantly, the reaction rates of the ferrous−oxy intermediate to oxidize L-Trp were increased with the electron-withdrawing ability of the heme substituents, implying that the more electron-deficient ferrous−oxy heme is favored for the PaTDO-catalyzed oxygenation. On the basis of these results, we propose that the initial step of the dioxygen activation by PaTDO is a direct electrophilic addition of the heme-bound O_2 to the indole ring of L-Trp.

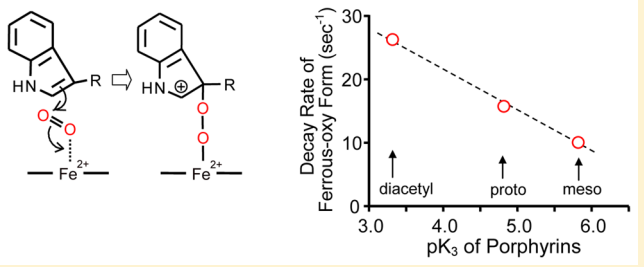

L-Tryptophan 2,3-dioxygenase (TDO) is a key enzyme that catalyzes the first step in the Trp catabolism of mammals and bacteria.[1−4] The enzyme inserts two oxygen atoms of O_2 into the pyrrole ring of L-Trp while forming *N*-formylkynurenine as a reaction product.[5] TDO exhibited higher specificity for the L-isomer of Trp but did not efficiently utilize other Trp analogues, including D-Trp as a substrate. Three decades after from the discovery of TDO, a second heme enzyme with the same Trp oxidative activity as that of TDO was found in rabbit small intestine.[6] This enzyme exhibited a much broader substrate specificity for several indoleamines, including D-Trp, and therefore was named indoleamine 2,3-dioxygenase (IDO).[7] The reaction mechanism of TDO isolated from *Pseudomonas acidovorans* was extensively studied by Ishimura et al., who detected the formation of the ferrous−oxy form in the steady state of the reaction and, subsequently, identified it as an obligate reaction intermediate.[8,9] A recent breakthrough in understanding the molecular basis of the heme-containing dioxygenase reactions was achieved via the crystallographic structures of recombinant human IDO and bacterial TDOs from *Xanthomonas campestris* and *Ralstonia metalliduran*.[10−12] These structural studies revealed that the catalytic sites were made by nonpolar amino acid residues, and the substrate Trp was located in a pocket over the distal side of the heme. The indole ring of Trp was perpendicular to the heme plane and bound close enough to the heme iron to allow O_2 insertion. Despite significant advances in structural characterization, the precise mechanism for the insertion of O_2 has yet to be established because of the lack of any information about peroxide intermediates, which are thought to be formed in steps subsequent to the formation of the ferrous−oxy form (Scheme 1).

Received: January 19, 2015
Revised: May 21, 2015
Published: May 21, 2015

DOI: 10.1021/acs.biochem.5b00048
Biochemistry 2015, 54, 3604−3616

Scheme 1. Reaction Mechanisms Proposed for Tryptophan Dioxygenase

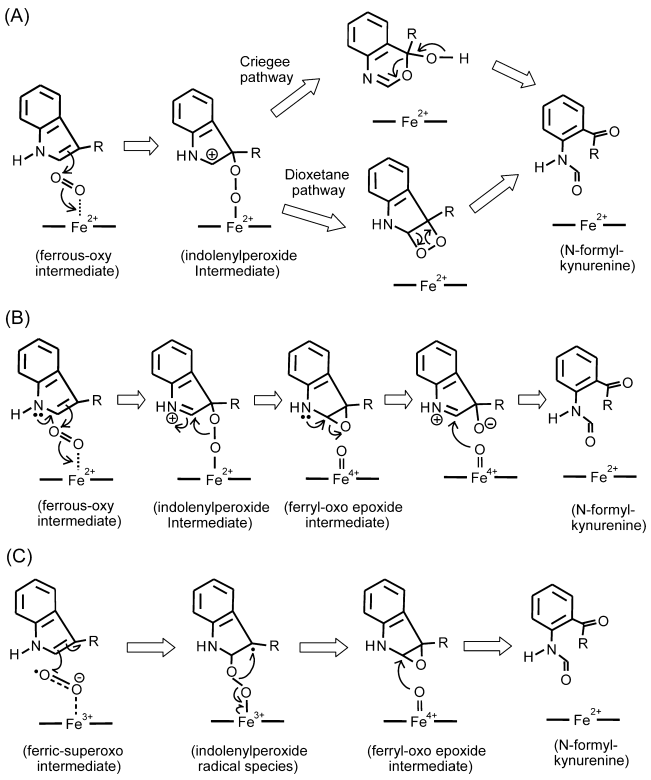

The first step of the TDO-catalyzed ring opening of L-Trp has been widely believed to be initiated by deprotonation of the indole NH of L-Trp by an active base.[13,14] Recent X-ray crystallographic studies proposed that a His residue (His55 in the XcTDO amino acid numbering) hydrogen bonding with the indole NH group served as the active base triggering the O_2 insertion.[11,12] Contrary to the expectation, the mutational studies did not support the mechanistic role of the His residue.[11,15] This led an alternate idea that the heme-bound O_2 serves as the active base, instead of the His residue.[15] However, this mechanism could not account for the experimental finding that 1-methyl-Trp with *N*-methylindole was considerably oxidized to *N*-formylmethylkynurenine.[16−18] Thus, mechanistic routes involving proton abstraction of the indole NH are thought to be unlikely, although still a matter of debate. An alternative pathway proposed for the key initial O_2 insertion step is a direct electrophilic addition of the heme-bound O_2 to the indole ring of L-Trp,[19,20] which does not require the proton abstraction of the indole NH (Scheme 1A). This electrophilic route favors the electron-deficient ferrous−oxy heme for the initial O_2 insertion. The indolenylperoxide intermediate, which was formed by direct electrophilic addition, converts to *N*-formylkynurenine via either the Criegee mechanism or the dioxetane mechanism (Scheme 1A). Neither of these mechanisms requires the changes in the oxidation state of the heme iron. In contrast, a recently proposed electrophilic route involved an epoxide species as a reaction intermediate, which was converted to the product by nucleophilic attack of the ferryl−oxo heme[21] (Scheme 1B). This pathway was inferred from the formation of cyclic aminoacetal as a byproduct derived from the ring opening of the epoxide intermediate.[21]

An alternative mechanism for the initial O_2 insertion step is a direct radical addition of the heme-bound O_2 with the electron-rich indole.[22−25] In this mechanism, the heme-bound O_2 in the ternary ferrous−oxy form is activated to $Fe^{3+}-O_2^-$ species and inserted into the $C_2{=}C_3$ bond of the indole ring by radical addition, to form an indolenylperoxide radical species (Scheme 1C). This species is subsequently converted to a ferryl−oxo epoxide intermediate via homolytic cleavage of the O−O bond, thereby allowing the insertion of two atoms of O_2 in a stepwise fashion. In the latter two pathways (Scheme 1B,C), the ferryl−oxo heme is involved as a reaction intermediate. Although several mechanistic pathways, including Scheme 1, have been proposed, there is no firm evidence for the electrophilic or radical mechanism in the enzymatic Trp dioxygenation.

In the electrophilic mechanism (Scheme 1A,B), the electron-deficient ferrous−oxy heme is favored to promote the initial step of the reaction, whereas the radical mechanism (Scheme 1C) requires the electron-rich ferrous−oxy heme (formulated as ferric−superoxo heme). The main factor in discriminating the electrophilic pathway from the radical pathway could be the difference in the electron density of the heme iron. A heme-modification approach described here could be the most appropriate way to uncover which of the electrophilic or radical pathways is the preferred route for the initial step of the O_2 insertion. This is because the heme-modification approaches allow us to control the electron density of the heme iron. For instance, replacements of the vinyl side chains at positions 2 and 4 of protoheme with alkyl or acyl groups largely changed the reactivities of hemoproteins such as peroxidase, myoglobin, and hemoglobin toward exogenous ligands.[26−29] These studies revealed that there was a linear free energy relationship between the affinity for exogenous ligands such as O_2 and the electron-withdrawing power of the heme substituents.[27−29] This provided robust evidence that the altered O_2 binding behaviors were primarily determined by the inductive electronic effects, rather than the steric effects of the heme substituents. The inductive effects were manifested almost entirely in the O_2 dissociation rate, which was influenced by the strength of the $Fe-O_2$ bond.[29] The difference in the $Fe-O_2$ bond strength is probably related to the difference in the electron density of the heme iron, as substantiated by the linear correlation between the redox potential of the enzymatic heme and the inductive effect of the heme substituents.[30] Thus, the interpretation based on these works is that the heme-modification approach focusing on the inductive electronic effects allows regulation of the partial electron donation from the heme iron to the heme-bound O_2.

In the heme-modification study presented here, we carefully checked the integrity of the enzymatic and structural properties of protoheme-reconstituted PaTDO by comparison with those of native PaTDO and then examined the inductive electronic effects of the heme substituents on the enzymatic and chemical properties of PaTDO by measuring the redox potentials of the heme, the infrared C−O vibrations, and the kinetic O_2 dissociation rates. These examinations strongly supported the possibility that the stronger electron-withdrawing effects of the heme substituents led to the more electron-deficient ferrous−oxy heme, probably by lowering the electron density of the ferrous heme iron. Finally, we found that the more electron-deficient ferrous−oxy heme was more active for Trp dioxygenation. These results led to the conclusion that the initial O_2 insertion catalyzed by PaTDO proceeds through electrophilic O_2 addition, while the radical addition mechanism may not be a preferred route. A portion of this work has been described previously.[31]

DOI: 10.1021/acs.biochem.5b00048
Biochemistry 2015, 54, 3604−3616

EXPERIMENTAL PROCEDURES

Reagents. L-Tryptophan was purchased from Wako Chemicals Co (Osaka, Japan) or Ajinomoto Co. Inc. (Tokyo, Japan). Research grade 1.26, 2.53, 5.02, or 9.90% O_2 gas balanced with N_2, and ^{14}NO gas, were obtained from Takachiho Chemical Co. (Tokyo, Japan). Deuteroheme IX was prepared from protoheme IX by the resorcinol melting method.[32] Mesoporphyrin IX was obtained from protoporphyrin IX by catalytic hydrogenation.[32] Mono- and diacetyldeuteroporphyrin IX were prepared by the slightly modified method described for the synthesis of dipropionyldeuteroporphyrin IX, in which anhydrous acetic acid was used instead of anhydrous propionic acid.[33] Diformyldeuteroporphyrin was synthesized using the previously described method.[28] These porphyrins were esterified by HCl/methanol and further purified by column chromatography.[33] The purified porphyrin dimethylesters were hydrolyzed in 6 N HCl at room temperature to produce corresponding porphyrins. The incorporation of iron into the porphyrins was achieved by the ferrous acetate method.[32]

Enzyme Purification. *P. acidovorans* (ATCC 11299b) was grown in a culture medium supplemented with L-Trp as an inducer.[34] L-Tryptophan 2,3-dioxygenase from the bacterial cells was purified at 4 °C in the presence of 5 mM L-Trp except for the HPLC chromatographic separations in the last two steps. Wet packed bacterial cells (200 g) suspended in 2 L of 50 mM KP_i buffer (pH 7.4), containing 2 mM ethylenediaminetetraacetic acid, 10 μM leupeptin, 2 μM pepstatin A, and 1 mM phenylmethanesulfonyl fluoride, were lysed with lysozyme (0.20 mg/mL). The cell lysate was treated by the addition of 1/10 volume of 5% streptomycin sulfate for 30 min to precipitate nucleic acid and was centrifuged at 13000*g* for 15 min to remove cell debris and nucleic acid. The resultant supernatant was concentrated to 100 mL using a Minitan ultrafiltration system (Millipore Japan, Tokyo, Japan) and then applied to a column of DEAE-cellulose A-500 (Seikagaku Kogyo, Tokyo, Japan) equilibrated with 40 mM KP_i buffer (pH 7.4). The enzyme was eluted with a linear NaCl gradient from 0 to 0.4 M in 40 mM KP_i buffer (pH 7.4). The active fractions were pooled and applied to a column of Ultrogel AcA 34 equilibrated with the same buffer containing 50 mM NaCl. The active fractions were collected and thoroughly washed with 40 mM KP_i buffer (pH 7.4) to remove NaCl and L-Trp using a Minitan ultrafiltration system. Then, the sample was applied to an L-Trp affinity column, in which the carboxyl group of L-Trp was conjugated to Sepharose 4B via four spacers. After the column was washed with the buffer containing 20 mM NaCl, protein was eluted with a 500 mL linear NaCl gradient from 0 to 0.2 M NaCl. The active fractions were pooled and applied to a Superdex 200pg column (26/600, GE Healthcare, Tokyo, Japan) connected to a Waters 600E HPLC system (Waters Japan, Tokyo, Japan). The elution of the enzyme was followed by simultaneously monitoring the absorbance at 406 and 280 nm. The collected sample was finally purified to an apparently homogeneous state with a Protein Pak G-DEAE HPLC column (Waters). The overall yield was ~24%. The resultant enzyme was stored in liquid nitrogen until it was used, after being equilibrated with 50 mM KP_i buffer (pH 7.4) containing 5% glycerol. The purity of the enzyme was estimated by SDS–PAGE. The enzyme preparation purified by this method is hereafter termed native PaTDO.

Preparation and Purification of Heme-Substituted PaTDO. Heme substitution was conducted by anaerobic heat treatment of the crude enzyme preparation in the presence of an excess amount of desired hemes. Such a heat treatment had been employed to remove undesired proteins in the original purification methods of PaTDO, in which excess protoheme was supplemented to prevent the formation of the apoenzyme.[34,35]

The extraction and the subsequent purification procedures of the enzyme were conducted at 4 °C, unless otherwise stated. The cell lysate from *P. acidovorans* (ATCC 11299b) grown in a medium containing L-Trp as an inducer was treated with streptomycin sulfate to remove nucleic acid. After removal of the cell debris and nucleic acid, the supernatant was followed by ammonium sulfate fractionation (240 g/L). The collected precipitates were dissolved in a minimal volume of 40 mM KP_i buffer (pH 7.4) with 5 mM L-Trp. After being diluted in 10 volumes of the same buffer, the enzyme solution was adsorbed onto a DE-52 cellulose column. The active enzyme fractions eluted by the linear NaCl gradient from 0 to 0.4 M in 40 mM KP_i buffer (pH 7.4) containing 5 mM L-Trp were concentrated and washed with 50 mM KP_i buffer (pH 7.4) with 0.4 mM L-Trp using an Amicon diaflow ultrafiltration apparatus (Millipore Japan). The resultant enzyme solution (~40 mL) was supplemented with the desired heme (1.4 mM) and subjected to heat treatment at 50 °C for 4 min in a water bath under anaerobic conditions. After being cooled in an ice bath, denatured proteins were removed by centrifugation. The enzyme was subsequently purified via Ultrogel AcA 34 gel filtration chromatography equilibrated with 50 mM KP_i buffer (pH 7.4) containing 50 mM NaCl and 5 mM L-Trp. The active fractions that eluted were finally purified by DE-52 cellulose chromatography to ensure the complete removal of the undesired residual heme bound to the protein. The overall yield was ~20%. The purified enzymes were stored in liquid nitrogen until they were used, after being equilibrated with 50 mM KP_i buffer (pH 7.4) containing 5% glycerol. All the heme-substituted PaTDOs catalyzed the O_2-dependent cleavage of L-Trp to *N*-formylkynurenine, of which production was confirmed by an increase in absorbance at 321 nm. The enzyme concentrations were expressed as heme concentration throughout this work and calculated using the following extinction coefficients at the Soret peak of the ferric enzyme in the absence of L-Trp: 157, 160, 170, and 100 mM^{-1} cm^{-1} for meso-, deutero-, proto-, and diacetyldeutero-PaTDO, respectively.

Preparations of Heme-Substituted Myoglobin and Cytochrome P450cam. The apoprotein of sperm whale myoglobin (Sigma) was prepared and reconstituted with synthetic hemes according to the method described previously.[27] The reconstitution of cytochrome P450cam with synthetic hemes was conducted by the method of Yu and Gunsalus.[36]

Spectral Measurements. Optical absorption spectra were recorded on a PerkinElmer Lambda 18 (PerkinElmer, Japan, Tokyo), a Union-Giken SM-401 (Unisoku Sci. Ins., Ibaraki, Japan), or a Shimadzu MPS-2000 (Shimadzu Co., Kyoto, Japan) spectrophotometer, equipped with a thermostatically controlled cuvette holder. EPR spectra were recorded on a Varian E-12 X-band spectrometer (Varian, Palo Alto, CA) with 100 kHz field modulation. The ferric enzymes employed for EPR measurements were prepared by adding a 2-fold excess of potassium ferricyanide to the L-Trp-free enzyme, and then the

DOI: 10.1021/acs.biochem.5b00048
Biochemistry 2015, 54, 3604–3616

residual ferricyanide was removed when the sample was passed through a Superdex 200HR HPLC column (GE Healthcare). The ^{14}NO adducts of the enzymes were prepared by flushing ^{14}NO gas to the ferrous enzyme, which were carefully reduced by adding a slight excess of sodium dithionite to the septum-sealed anaerobic EPR tubes. Infrared spectra were measured on a Jasco IR-810 spectrophotometer with a CaF_2 cell with a light path length of 0.1 mm. The temperature of the cell was controlled with thermomodule elements attached to the cell holder.

Oxidation−Reduction (Redox) Potential Measurements. The redox potentials were measured by a potentiometric titration using sodium dithionite as a reductant and potassium ferricyanide as an oxidant.[34] L-Trp included in the stored protein samples was removed by passing samples through a Sephadex G-25 column (GE Healthcare). Mediators were a mixture of 3 μM thionine (+64 mV), 4 μM pyocyanine (−34 mV), 3 μM 2,6-dichloroindophenol (+215 mV), 10 μM 2,6-dichlorophenol indo-*o*-cresol (+180 mV), and 4 μM toluylene blue (+115 mV). The electrode was calibrated with myoglobin. Redox potential was quoted versus the normal hydrogen electrode (NHE).

Stopped-Flow Measurements. The binding of O_2 to the ferrous enzymes was analyzed by a Union-Giken rapid scan stopped-flow spectrophotometer (model RA-401) equipped with a photodiode array detector. The ferric reconstituted PaTDOs in one reservoir were photoreduced under anaerobic conditions by illuminating 150 W white light in the presence of 1 mM ethylenediaminetetraacetic acid and 0.3 μM flavin adenine dinucleotide phosphate. The desired O_2-dissolved buffer solutions in the other reservoir were prepared by bubbling 2.53, 5.02, and 9.90% O_2 gas (balanced with N_2) or air for 10 min. The pseudo-first-order rate constants were determined by a single-exponential analysis using GraphPad Prism. The O_2 association rate constant (k_{on}) and O_2 dissociation rate constant (k_{off}) were determined from the slopes and the *y*-axis intercepts, respectively, in the plots of the pseudo-first-order rate constants versus O_2 concentration. The data are an average of four or five measurements and presented with the standard error of the mean.

The decay rates of the ternary ferrous−oxy forms under the catalytic conditions were determined by the stopped-flow spectrophotometer at 20 °C. The one reservoir included the photoreduced enzymes in the anaerobic buffer solution and the other the O_2 solution equilibrated with pure O_2 gas (1.2 mM O_2). The buffer solutions in both reservoirs contained 10 mM L-Trp. The level of the ferrous−oxy heme formed under steady state conditions was estimated as described elsewhere.[9] In brief, the initial absorbance changes in the formation of the ferrous−oxy form after mixing were measured as a function of O_2 concentration. Then, the full conversion into the ferrous−oxy heme at infinite O_2 concentration was estimated by a hyperbolic regression analysis of the plots between the observed absorption increases and the initial O_2 concentrations. The decay rate constants of the ferrous−oxy forms, which corresponded to k_{cat}, were determined by dividing the initial O_2 concentration by the area under stopped-flow trace:[9,37] $k_{cat} = [O_2]/\int ES\, dt$, where ES represents the ferrous−oxy form. The areas were calculated using GraphPad Prism.

Resonance Raman Measurements. The resonance Raman spectra were recorded with a Jasco NR-1800 spectrometer equipped with a liquid nitrogen-cooled CCD detector (Princeton Instruments). The excitation wavelength was a 413.1 nm line from a Krypton ion laser (Coherent, Innova 90). Calibration of the Raman line was performed using indene.

Activity Measurements. The TDO activity was determined spectrophotometrically by monitoring the production of *N*-formylkynurenine at 321 nm (ε = 3750 M^{-1} cm^{-1}). In the process of enzyme purification, the assays were conducted in a mixture containing 50 mM KP_i buffer (pH 7.4), 4 mM L-Trp, 1.3 mM sodium ascorbate, and the enzyme in a total volume of 2.5 mL at 20 °C. In the determinations of K_m for O_2, the ferrous enzymes were generated by photoreduction in the presence of 1 mM L-Trp as described in a preceding section and were added to the reaction mixtures with a gastight syringe. Under the conditions, the level of product formation linearly increased without showing a lag period. The K_m for O_2 was determined by one-site binding hyperbola analyses using GraphPad Prism. The results are presented with the standard error of the mean.

Determinations. Protein was determined by a modified biuret method of Yonetani[38] or BCA protein assay (Thermo Scientific) using bovine serum albumin as a standard. The heme content was quantified by the pyridine hemochrome method. The purities of native and reconstituted PaTDO were estimated by SDS−PAGE. Protein was visualized by Coomassie blue staining. To estimate the purities of reconstituted enzymes, protein bands were digitized by a Typhoon FLA 9500 imager and their band intensities quantified with ImageQuant (version 5.2).

RESULTS

Enzymatic Properties of Native and Protoheme-Reconstituted PaTDO. Although protoheme in PaTDO could be readily removed by acid−acetone or acid−methylethylketone treatment, the reconstitution of the enzymatically active PaTDO from the resultant apoprotein and protoheme was unsuccessful. In this study, the enzymatic protoheme was successfully replaced with synthetic hemes when the crude enzyme preparations were subjected to heat treatment in the presence of an excess of the desired heme. Such a reconstitution procedure may arouse concerns regarding the integrity of the enzymatic properties. To ensure the structural integrity of the reconstituted enzymes, the spectral properties of the protoheme-reconstituted enzyme were compared with those of native PaTDO, which was purified by a mild method as described in Experimental Procedures.

Native PaTDO in the ferric state showed the optical spectrum with absorption maxima at 405, 502, and 632 nm and an axial symmetric EPR signal centered around g = 5.8 in the absence of L-Trp (Figure 1A,B). These spectroscopic features were indicative of a typical six-coordinate high-spin ferric heme with a H_2O molecule at the sixth coordinate position of the heme. Essentially the same optical and EPR spectral characteristics were identified for the protoheme-reconstituted PaTDO (Figure S1 of the Supporting Information and ref 34). The ferrous form of native PaTDO exhibited a high-spin spectrum with 433 and 554 nm bands (Figure 1A), consistent with that of the protoheme-reconstituted ferrous PaTDO (Figure S1 of the Supporting Information). These spectroscopic observations indicate that the heme coordination structure of the protoheme-reconstituted PaTDO remains intact.

The reliability was further confirmed by examining the enzymatic properties. The native PaTDO preparations

DOI: 10.1021/acs.biochem.5b00048
Biochemistry 2015, 54, 3604−3616

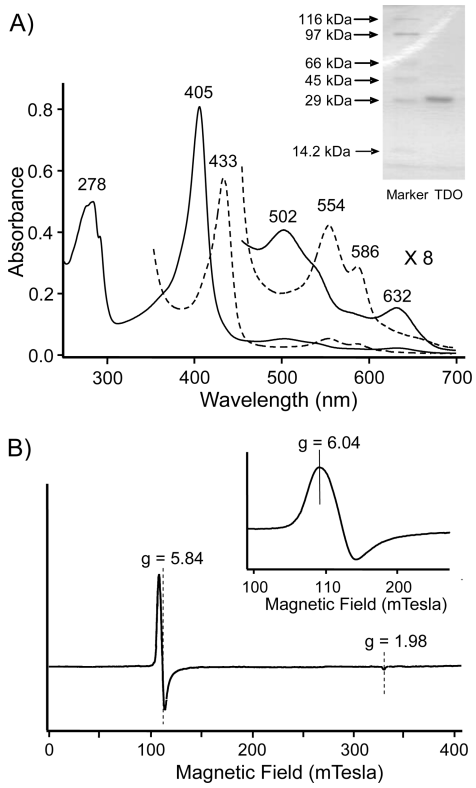

Figure 1. Optical and X-band EPR spectra of native PaTDO. (A) Optical spectra were recorded in 50 mM KP_i buffer (pH 7.0) in the absence of L-Trp at 20 °C. The ferrous enzyme was prepared by the addition of $Na_2S_2O_4$. The solid and dashed lines denote data for the ferric and ferrous enzymes, respectively. In the inset, SDS–PAGE (10% running gel) of the purified enzyme is shown. (B) X-Band EPR spectrum at 5 K in 50 mM KP_i buffer (pH 7.0) in the absence of L-Trp. In the inset, the signal around $g = 6$ is shown on an expanded scale. The enzyme concentration was ~90 μM as heme.

exhibited a specific activity of ~22 μmol of product min^{-1} (mg of protein)$^{-1}$ and a maximal turnover number per heme between 950 and 1050 min^{-1}. These enzymatic activities were comparable to those of the protoheme-reconstituted PaTDO, which exhibited a specific activity of 14–16 μmol of product min^{-1} (mg of protein)$^{-1}$ and a maximal turnover number per heme of 900–1000 min^{-1}. In addition, the enzymatic activities of native and protoheme-reconstituted enzymes described here essentially agreed with those of the preparations obtained by the original purification method.[34,35,39]

SDS–PAGE analyses indicated that native TDO gave a nearly homogeneous single protein band with a mass of 29.5 kDa (inset of Figure 1A). Likewise, the protoheme-reconstituted enzyme gave a major protein band with a mass of 29.5 kDa (inset in Figure S1 of the Supporting Information). In addition to the major band, an ~45 kDa band was identified as an impurity and estimated to be 16 ± 2% of total protein by the method described in Experimental Procedures. The gel filtration chromatographic analyses showed that the molecular mass of native PaTDO was approximately 115 kDa (data not shown), composed of tetramer of a 29.5 kDa subunit. The heme contents of native and protoheme-reconstituted enzymes were 2.10 ± 0.14 and 2.20 ± 0.17 hemes/tetramer, respectively. Both enzyme preparations displayed sigmoidal kinetics with respect to Trp (Hill coefficient of ~2.4). The sigmoidal kinetics was transformed to the Michaelis–Menten kinetics upon addition of α-methyltryptophan, which did not act as either substrate or competitive inhibitor. On the basis of the results, one may propose that subunits without heme might serve as allosteric subunits that can bind α-methyltryptophan as well as Trp. These results, including the heme content, essentially agree with that reported for the heat-treated preparation[40,41] and indicate that the heat treatment has practically no effect on the protein architecture of PaTDO.

Using the native and protoheme-reconstituted PaTDO, we measured their EPR and resonance Raman spectra to characterize their fifth ligand. As shown in Figure 2A, the

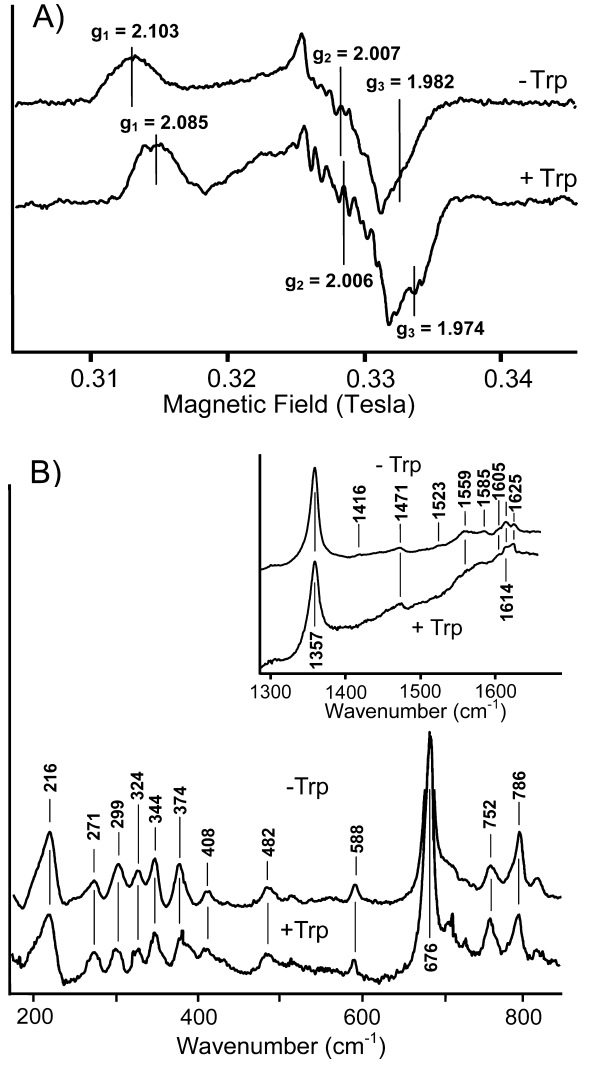

Figure 2. Spectroscopic analyses of the proximal ligand of native PaTDO. (A) X-Band EPR spectra of ^{14}NO adducts in the absence and presence of 4 mM L-Trp at 35 K. (B) Resonance Raman spectra of native ferrous PaTDO. The excitation wavelength was 413.1 nm, and the laser power was ~10 mW. In Raman experiments, the enzyme (~40 μM as heme) was dissolved in 50 mM KP_i buffer (pH 7.4) in the absence and presence of 4 mM L-Trp.

ferrous NO adducts of native PaTDO exhibited EPR signals characteristic of a six-coordinate ferrous ^{14}NO heme with a superhyperfine splitting in the central signal around $g = 2$ in the absence and presence of L-Trp. The superhyperfine structure of a triplet of triplets was an indication of an axial ligand with ^{14}N nuclei, a His residue,[42] as has been shown by the previous EPR examination.[43] The slight modification of the superhyperfine

DOI: 10.1021/acs.biochem.5b00048
Biochemistry 2015, 54, 3604–3616

structure upon addition of Trp suggested a small geometrical change in NO coordination, although details were unknown.

Resonance Raman experiments provided further evidence of the ligation of His at the proximal position of the heme (Figure 2B). The ferrous form of native PaTDO showed a distinct Fe–His Raman band at 216 cm^{-1} both in the absence and in the presence of L-Trp. The corresponding Raman band of protoheme-reconstituted PaTDO was identified as the 213 cm^{-1} band (data not shown). The observed Fe–His Raman frequency at 216 cm^{-1} is significantly lower than that of HRP with an anionic imidazolate His, indicating that the proximal His residue of PaTDO is neutral. Furthermore, the resonance Raman data revealed that the enzymatically active ferrous form of PaTDO has a five-coordinate high-spin heme, as indicated by the ν_4 band at 1357 cm^{-1} and the ν_3 band at 1471 cm^{-1} (inset of Figure 2B). These results together with optical spectroscopic observations demonstrate that the ferrous heme in native and protoheme-reconstituted PaTDO is a five-coordinate high-spin form with a neutral His as the proximal ligand.

Electronic Properties of Porphyrin Substituents. The side chains of synthetic porphyrins employed in this study differed in their electron-withdrawing nature from the vinyl side chains of protoporphyrin IX (Figure 3). For instance, the ethyl

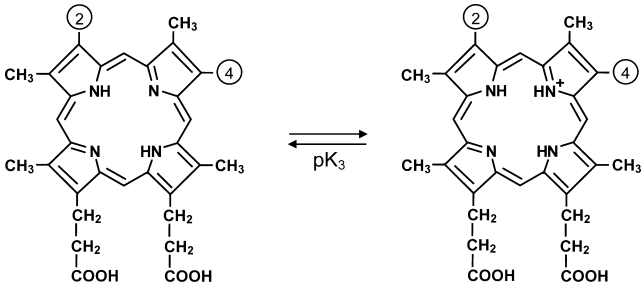

Porphyrins	Substituents in positions 2	4	pK_3
Meso	CH_2CH_3	CH_2CH_3	5.8
Deutero	H	H	5.5
Proto	$CH=CH_2$	$CH=CH_2$	4.8
2 (or 4)-Monoacetyldeutero	$CO-CH_3$ or H	H or $CO-CH_3$	4.2
2,4-Diacetyldeutero	$CO-CH_3$	$CO-CH_3$	3.3
2,4-Diformyldeutero	CHO	CHO	3.0

Figure 3. Chemical structures of porphyrins and their pK_3 values. The substituents at positions 2 and 4 are indicated in the figure. The pK_3 values of porphyrins, which correspond to the −logarithm of K_d between the neutral and monocation form of porphyrins, were taken from ref 44.

side chains of mesoporphyrin are less electron-withdrawing than the vinyl side chains of protoporphyrin, whereas the acetyl side chains have greater electron-withdrawing ability. Such an inductive electron-withdrawing nature is reflected in their pK_3 values of corresponding porphyrins, which referred to a proton dissociation constant between neutral and monocation states of porphyrins[44] (Figure 3). The pK_3 value becomes smaller with the increasing order of the electron-withdrawing power and has been used as an index of the inductive electronic effects (Figure 3). In the heme-modification study presented here, mesoheme, protoheme, and diacetyldeuteroheme were selected to examine the heme substituent effects. The difference of 2.5 in the pK_3 value between diacetyldeuteroporphyrin and mesoporphyrin is sufficiently large to assess the inductive electronic effects. Although one may point out that the size and shape of the substituents of diacetyldeuteroheme are different from those of other two hemes, the use of diacetyldeuteroheme is indispensable and still useful for assessing a relationship between the inductive electronic effects of the heme substituents and the altered functional behaviors of reconstituted TDO. In some cases, data of deuteroheme-reconstituted TDO were included to reinforce the conclusion, although the data were limited by the difficulty of reconstitution. For measurements required to draw a key conclusion, the relationships between the altered functional behaviors and the heme substituent effects were completed by using data of reconstituted myoglobin and cytochrome P450cam with widely different inductive effects of the heme substituents.

Enzymatic and Optical Spectral Properties of Reconstituted PaTDOs. The heme content of reconstituted enzymes was determined on the basis of SDS–PAGE analyses as described in Results. As mentioned for protoheme-reconstituted PaTDO, the 29.5 kDa band in the SDS–PAGE gel was identified as a major protein band for all reconstituted enzymes: 74, 62, and 67% for meso-, deutero-, and diacetyldeutero-TDO, respectively. The calculated heme contents were 2.25 ± 0.15, 1.97 ± 0.15, and 2.32 ± 0.21 hemes/tetramer for meso-, deutero-, and diacetyldeutero-TDO, respectively. The maximal specific activities were 10.4, 12.7, and 24.7 μmol min^{-1} (mg of protein)$^{-1}$ for meso-, deutero-, and diacetyldeutero-TDO, respectively. Pyridine hemochrome assays indicated that the meso- and diacetyldeutero-PaTDOs contain no measurable amount of protoheme, while the deuteroheme-substituted enzyme retained a small amount of protoheme (~10%) (data not shown).

Optical spectra of heme-substituted PaTDOs in the ferric and ferrous states are summarized in Figure 4. The Soret peak positions of meso- and deutero-PaTDO in the ferric and the ferrous states were blue-shifted relative to those of proto-PaTDO. In contrast, diacetyldeutero-PaTDO displayed a red-shifted Soret peak in the ferric and ferrous states. These peak positions were comparable to those of reconstituted myoglobin or HRP containing the corresponding hemes.[27] These optical spectral features show that the ferric forms of all heme-substituted PaTDOs are in a six-coordinate high-spin state, and the ferrous forms are in a five-coordinate high-spin state.

Midpoint Potentials (E_m) of Heme-Substituted PaTDOs. The midpoint potential (E_m) measurements for the ferric/ferrous couple are the most sensitive approach to estimate the relative electron density of the heme iron. Figure 5 shows the potentiometric titration data of the heme-substituted PaTDOs in the absence of L-Trp. In both reductive and oxidative titrations, the spectra changed through one set of isosbestic points (Figure S2 of the Supporting Information). The data were fitted to a single-electron redox equilibrium to determine the E_m of the enzymatic hemes. The E_m of the protoheme-reconstituted enzyme was +82 mV, which was slightly lower than the previous value (+100 mV at pH 7.4).[27] Diacetyldeutero-PaTDO gave an E_m of +150 mV, which was substantially higher than that of proto-PaTDO. In contrast, the E_m values of deutero- and meso-PaTDO were lowered to +55 and +32 mV, respectively. As shown in the inset of Figure 5, there is an essentially linear correlation between E_m values and pK_3 of metal-free porphyrins. A similar correlation was also

DOI: 10.1021/acs.biochem.5b00048
Biochemistry 2015, 54, 3604–3616

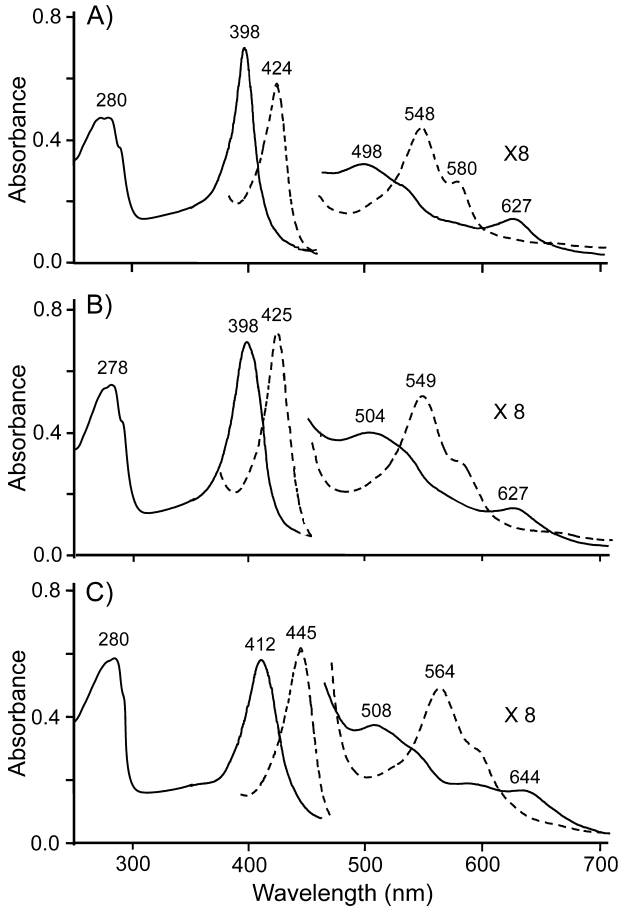

Figure 4. Optical absorption spectra of reconstituted PaTDOs. Optical spectra of (A) meso-PaTDO, (B) deutero-PaTDO, and (C) diacetyldeutero-PaTDO, in the absence of L-Trp at 20 °C. Solid and dashed lines show data the ferric and ferrous enzymes, respectively. In all cases, spectra in the visible region are illustrated on an expanded scale (8×). The buffer was 50 mM KP_i buffer (pH 7.4).

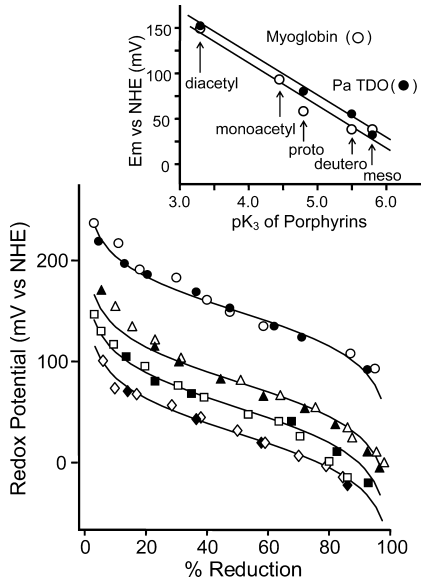

Figure 5. Potentiometric titrations of the heme redox potential at 20 °C. The reaction mixture was composed of ~15 μM heme-substituted PaTDOs in 50 mM KP_i buffer (pH 7.4). The empty and filled symbols denote the data determined by reductive and oxidative titrations, respectively. Circles, triangles, squares, and diamonds denote data points for diacetyl-, proto-, deutero-, and meso-PaTDO, respectively. In the inset, the midpoint potential of each heme-substituted enzyme is plotted vs pK_3 of porphyrins (●). For comparison, the midpoint potentials of heme-substituted myoglobins at pH 5.5 are also plotted vs pK_3 in the inset (○).

established for heme-substituted myoglobins (inset of Figure 5). These results together with a previous study[30] indicate that increasing the extent of electron withdrawal of the heme substituents stabilizes the ferrous enzymatic heme, as a result of a decrease in the electron density of the enzymatic heme.

Effects of Heme Substituents on the C−O Vibration. CO binds to the heme iron via the formation of the σ bond, which donates electrons to the heme iron from CO. The increased electron on the heme iron associated with the σ bond formation is donated to the vacant $p\pi^*$ orbital of CO to stabilize the Fe−CO unit. This is termed π back-donation. Thus, the C−O stretching vibration of the heme-bound CO is sensitive to the electron density of the heme iron and is helpful in the evaluation of the inductive electronic effects of the heme substituents. The infrared C−O stretching bands of the heme-substituted PaTDOs are shown in Figure 6A. The C−O stretching frequency (νC−O) of proto-PaTDO at 1969 cm^{-1} agreed with that of previous report.[45] The data tended to exhibit a higher frequency shift of the νC−O with a decrease in pK_3 of porphyrins (Figure 6B). The linear correlation between νC−O and pK_3 was established using reconstituted myoglobins (Figure 6B).

Uchida et al. found that the C−O stretch of the substrate-free PaTDO exhibited a broad band that consisted of two components, which converted to a sharp single band with an apparent half-bandwidth of 10 cm^{-1} in response to L-Trp binding.[45] The L-Trp-induced narrowing in the half-bandwidth may reflect the conformational freedom of the bound CO.[46] The bandwidth of the C−O stretching vibrations of meso- and proto-PaTDO in the presence of L-Trp was 10 cm^{-1}, while that of diacetyldeutero-PaTDO was slightly broader (~13 cm^{-1}). This point will be discussed later.

Effects of the Heme Substituent on the Formation of the Ferrous−Oxy Form. Analyses of the binding of O_2 to the ferrous heme iron of PaTDO should be quite important for gaining insight into the effects of the heme substituent on the O_2 activation mechanism. The O_2 binding kinetics of the ferrous PaTDO conformed to a single-exponential process in the presence of an excess of O_2 and L-Trp (Figure S3 of the Supporting Information). The pseudo-first-order rate constants thus obtained were plotted against the O_2 concentration to determine kinetic rate constants for O_2 association and O_2 dissociation (inset of Figure S3 of the Supporting Information). As shown in Figure 7A, the O_2 association rate constant (k_{on}) of proto-PaTDO [$(3.6 \pm 0.1) \times 10^6$ M^{-1} s^{-1}] was essentially the same as that of meso-PaTDO [$(3.6 \pm 0.2) \times 10^6$ M^{-1} s^{-1}], while that of diacetyldeutero-PaTDO was slightly smaller [$(1.1 \pm 0.1) \times 10^6$ M^{-1} s^{-1}]. In contrast to k_{on}, the dissociation rate constants for O_2 (k_{off}) increased in the following order: 83.1 ± 8.4, 111.6 ± 8.2, and 144.8 ± 10.9 s^{-1} for meso-, proto-, and diacetyldeutero-PaTDO, respectively (Figure 7B). This suggests that the inductive electronic effects of the heme substituents are dominantly reflected on the O_2 dissociation reaction, rather than the O_2 association reaction.

We attempted to substantiate this prediction by using heme-substituted cytochrome P450cam. This hemoprotein was chosen with the aim of extracting the intrinsic effects of the

DOI: 10.1021/acs.biochem.5b00048
Biochemistry 2015, 54, 3604−3616

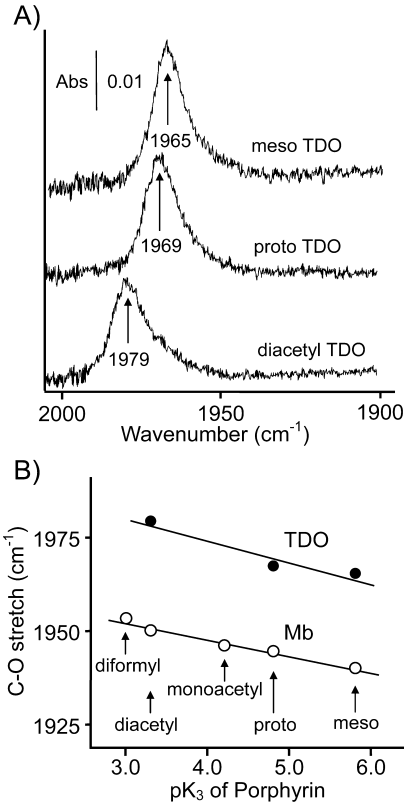

Figure 6. Infrared spectra of the CO complex of heme-substituted PaTDOs. The CO adducts were prepared by adding sodium dithionite to the CO-saturated enzyme solutions. (A) Infrared spectra were measured in 50 mM KP_i buffer (pH 7.4) containing 10 mM L-Trp at 15 °C. The concentrations of the enzymes were 860, 780, and 750 μM for meso-, proto-, and diacetyldeutero-TDO, respectively. (B) Plot of C−O stretching frequencies vs pK_3 of porphyrins (●). To establish a linear correlation between the C−O stretch and pK_3, C−O stretching frequencies of heme-substituted CO-myoglobins at pH 7.0 are plotted (○).

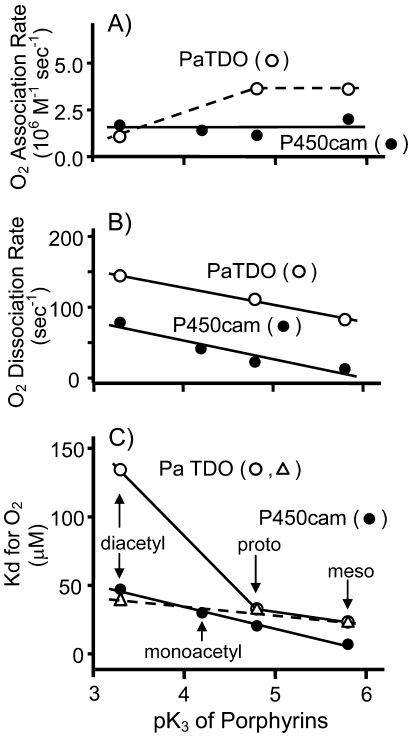

Figure 7. Oxygen binding parameters (k_{on}, k_{off}, and K_d) of heme-substituted PaTDO and cytochrome P450cam plotted vs the pK_3 of porphyrins. Data were collected at 10 and 15 °C for PaTDO and P450cam, respectively. Empty and filled circles denote data points for PaTDO and P450cam, respectively. (A) Oxygen association rate constants (k_{on}) for each enzyme plotted vs the pK_3 of porphyrins. (B) Oxygen dissociation rate constants (k_{off}) for each enzyme plotted vs the pK_3 of porphyrins. (C) O_2 dissociation constants (K_d) that were calculated by dividing k_{off} by k_{on} plotted vs the pK_3 of porphyrins. Empty triangles are predicted data points for PaTDO, where k_{on}, the rate of diacetyldeutero-PaTDO, was thought to be essentially the same as that of proto- and meso-PaTDO. In panels A and B, the k_{on} and k_{off} were determined using a stopped-flow apparatus at the various oxygen concentrations, in the presence of 10 mM Trp and 1 mM d-camphor for PaTDO and P450cam, respectively. Cytochrome P450cam was reduced by a sight excess of NADH in the presence of catalytic amounts of putidaredoxin and putidaredoxin reductase under anaerobic conditions.

inductive electronic property on the O_2 binding reaction, because it has a rigid and vacant pocket large enough to accommodate an O_2 molecule that minimizes the steric interaction with nearby amino acid residues and/or a substrate camphor in the O_2 binding site.[47] The electronic effects of the heme substituents exert essentially no effect on k_{on} for O_2 ($1.2-2.0 \times 10^6$ M^{-1} s^{-1}) as summarized in Figure 7A, while the k_{off} for O_2 increases rigorously depending on an increase in the electron-withdrawing effects: 13.5 ± 3.7, 23.2 ± 3.7, 41.9 ± 5.5, and 79.0 ± 6.5 s^{-1} at 15 °C for meso-, proto-, monoacetyldeutero-, and diacetyldeutero-P450cam, respectively. As described below, the reliability of k_{off} for O_2 in the case of TDO was checked by an indirect method.

As shown in Figure 7B, the O_2 dissociation rate constants inversely correlate with pK_3 in both heme-substituted enzymes. These data reveal that the O_2 dissociation is affected by the strength of the Fe−O_2 bond and support the idea that the weaker π back-donation from the heme iron to the O_2 moiety promotes the formation of the electron-deficient ferrous−oxy heme.[48−50]

The oxygen affinities (K_d for O_2) for the heme-substituted PaTDO and P450cam were calculated by dividing k_{off} by k_{on}. The calculated O_2 affinities of the heme-substituted PaTDO decrease in the increasing order of the electron-withdrawing effects of the heme-substituents: 23.1, 31.0, and 131.6 μM for meso-, proto-, and diacetyldeutero-PaTDO, respectively. Likewise, the O_2 affinities for heme-substituted P450cam decrease in the same trend: 6.7, 20.2, 29.7, and 46.8 μM for meso-, proto-, monoacetyldeutero-, and diacetyldeutero-P450cam, respectively. A linear correlation between the O_2 affinity and pK_3 of porphyrins was established for cytochrome P450cam (Figure 7C), while PaTDO lacked a linear correlation against pK_3 of porphyrins (Figure 7C). This might be due to the effect of other factors such as size and/or hydrophilic effect of acetyl side chains. If the k_{on} rate of O_2 for diacetyldeutero-TDO is thought to be unaltered by such effects and the resultant k_{on} rate is essentially equivalent to those of meso- and proto-TDO, the K_d for diacetyldeutero-TDO is calculated to be 40 μM. When this predicted value was plotted against pK_3, an essentially linear relationship was observed (dashed line in Figure 7C). These suggest that access of O_2 to the Fe atom of diacetyldeutero-TDO was sterically hindered and substantiates the idea that the O_2 dissociation rate was a significant measure of back-bonding strength between O_2 and heme iron.[51]

DOI: 10.1021/acs.biochem.5b00048
Biochemistry 2015, 54, 3604−3616

It is not possible to directly measure the O_2 dissociation rate from ferrous−oxy TDO, because the ferrous−oxy TDO is solely observable under the steady state condition in the presence of L-Trp and very unstable in the absence of L-Trp. To verify the reliability of the k_{off} value, we attempted to measure K_d for O_2 by an alternative method. As summarized in Figure S4 of the Supporting Information, the maximal level of the ferrous−oxy form of reconstituted PaTDO in the presence of a variable amount of O_2 was measured under stopped-flow conditions and plotted as a function of O_2 concentration. The relationship between the level of the ferrous−oxy form and O_2 concentration was hyperbolic. The calculated K_d values were 25.6 ± 2.1, 36.7 ± 2.7, and 142 ± 15.6 μM for meso-, proto-, and diacetyldeutero-TDO, respectively, and essentially agreed with K_d values obtained from k_{off}/k_{on}. This assures the reliability of k_{off} values, which was obtained from Figure S3 of the Supporting Information.

Effects of the Heme Substituent on the K_m for O_2 and Catalytic Activities. The relations between the initial rates of *N*-formylkynurenine formation and variable O_2 concentrations conform to the simple Michaelis−Menten type kinetics (Figure S5 of the Supporting Information). The K_m for O_2 calculated from Figure S5 of the Supporting Information increased with the electron-withdrawing ability of the heme substituents: 20.3 ± 1.4, 30.2 ± 2.9, 34.5 ± 2.1, and 172.7 ± 12.0 μM for meso-, deutero-, proto-, and diacetyldeutero-PaTDO, respectively. These K_m values virtually agreed with the O_2 affinity (K_d for O_2) for corresponding heme-substituted PaTDO. Comparison of the O_2 affinities with the K_m values for O_2 confirms that the reactants (Trp−TDO complex and O_2) and the ternary ferrous−oxy intermediate (Trp−ferrous−oxy form) are at rapid equilibrium, and the decay of the ternary ferrous−oxy form is a rate-limiting step in the enzymatic reactions, regardless of the difference in the electronic effects of the heme substituents.

The enzymatic activities (k_{cat}) determined by the overall kinetics were 580 and 650 min^{-1} for meso-TDO, 1000 and 1040 min^{-1} for deutero-TDO, 900 and 950 min^{-1} for proto-TDO, and 1550 and 1750 min^{-1} for diacetyldeutero-TDO (for two separate preparations of each heme-substituted enzyme). When these data were plotted against pK_3 of porphyrins, the dioxygenase activity exhibited an increased trend with the electron-withdrawing ability of the heme substituents (Figure 8A).

To confirm the findings described above, we directly determine the rate constants (k_{cat}) from the decay process of the ternary ferrous−oxy form in the presence of 10 mM L-Trp and 0.6 mM O_2. Data obtained using a rapid scan stopped-flow apparatus are summarized in Figure 9. The ternary ferrous−oxy intermediates were immediately formed after mixing (Figure 9A,B). The Soret peaks of the ferrous−oxy forms were 408, 417, and 427 nm for meso-, proto-, and diacetyldeutero-PaTDO, respectively, which essentially agreed with those of oxymyoglobins containing corresponding heme.[27] Under the experimental conditions, the ferrous forms of meso- and proto-PaTDO almost entirely converted to the ferrous−oxy form, while the conversion of ferrous diacetyldeutero-PaTDO was incomplete. This partial conversion of diacetyldeutero-PaTDO is due to the low O_2 affinity as mentioned previously. The ternary ferrous−oxy forms gradually converted to the ferrous forms as shown in Figure 9B, wherein the conversion was ensured by the formation of the ferrous enzyme immediately after the reactions were completed (Figure 9A). The decay

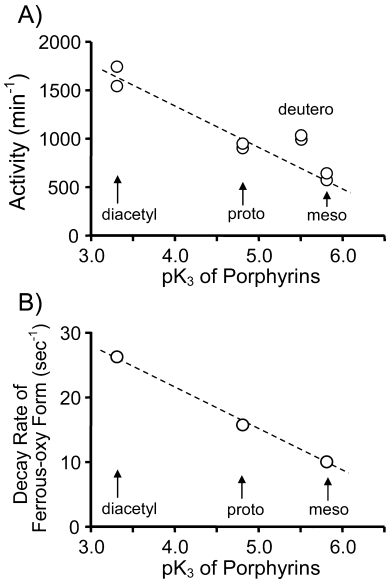

Figure 8. Plots of dioxygenase activities vs pK_3 of porphyrins. (A) Maximal turnover number per heme obtained from two separate preparations of each heme-substituted enzyme plotted vs the pK_3 of porphyrins. The initial rates for the formation of *N*-formylkynurenine were determined at 321 nm in the presence of 20 mM L-Trp and 1.2 mM O_2 at 20 °C. (B) Decay rates (k_{cat}) of the ternary ferrous−oxy forms of the heme-substituted enzymes, which were determined as described in the legend of Figure 9, plotted vs the pK_3 of porphyrins.

rates of the ferrous−oxy form (k_{cat}), which were determined as described in Experimental Procedures, were 10.2 ± 0.4, 15.9 ± 0.7, and 26.3 ± 2.5 s^{-1} for meso-, proto-, and diacetyldeutero-PaTDO, respectively (i.e., ∼610, ∼950, and ∼1580 min^{-1} for meso-, proto-, and diacetyldeutero-PaTDO, respectively). Each value essentially agreed with the k_{cat} value obtained by overall kinetics for the corresponding heme-substituted PaTDO. The k_{cat} values tended to linearly increase with an increase in the electron-withdrawing power of the heme substituents (Figure 8B). These results together with the effects of the heme substituents on the O_2 dissociation rates suggest that the greater electron-deficient ferrous−oxy heme is more active for the insertion of O_2 into the indole ring of L-Trp. This mechanistic proposal accounts for the reason why the electron-rich 5- or 6-methyl-D,L-Trp with an electron-donating methyl group on the indole benzene ring was a good substrate for both human IDO and XcTDO as compared with unsubstituted Trp.[14,15,52]

■ DISCUSSION

Effects of Chemical Properties of Heme Substituents on Heme Coordination. As mentioned above, studies of chemical modification of vinyl side chains at positions 2 and 4 of protoheme on hemoprotein functions demonstrated that the altered functional behaviors by heme modification had its origin in the inductive electronic effect, rather than the steric effect of the heme substituents.[27−29]

In this study, we applied this technique to analyze the reaction mechanism of PaTDO. Although we have no available information for the active site structure of PaTDO, it is known that in the crystal structure of tetrameric XcTDO, the vinyl side chains of the protoheme are surrounded and interacted with Phe51, His55, and Tyr113, and also with Tyr24, which is a residue from another monomer of the tetramer.[11] Because

DOI: 10.1021/acs.biochem.5b00048
Biochemistry 2015, 54, 3604−3616

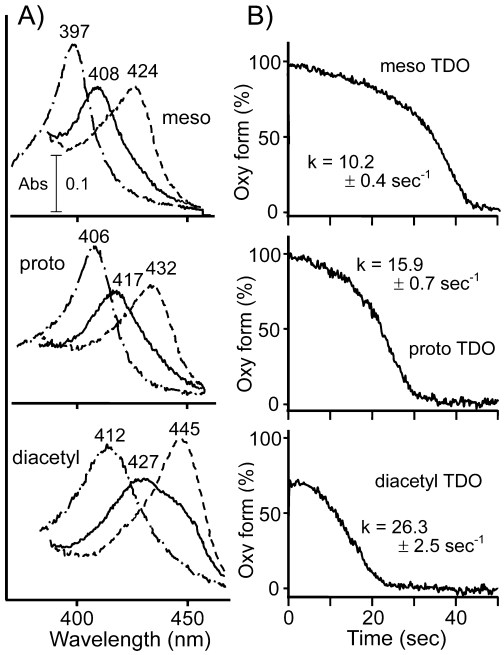

Figure 9. Spectrophotometric detections of ternary ferrous−oxy forms and determinations of their decay rates under catalytic conditions. (A) Optical spectra illustrated by solid, chain, and dashed lines denote those of the ferrous−oxy form, the ferric form, and the ferrous form of the heme-substituted PaTDOs (meso-, proto-, and diacetyldeutero-PaTDO from the top), respectively. Spectra of the ferrous−oxy form were recorded at 20 ms after mixing. (B) Decay of the ferrous−oxy forms to the ferrous forms was monitored at 407, 415, and 422 nm for meso-, proto-, and diacetyldeutero-TDOs, respectively. The amounts of the ternary ferrous−oxy forms and the decay rates were calculated as described in Experimental Procedures. The final enzyme concentrations were 2.03, 1.84, and 3.01 μM for meso-, proto-, and diacetyldeutero-TDO, respectively.

these active site residues are highly conserved among members of the TDO family, it is likely to consider that vinyl groups of protoheme in PaTDO interact with the analogous residues. When the synthetic hemes were incorporated into the heme pocket of PaTDO, in place of the protoheme, substituents at positions 2 and 4 might interact with these residues, eventually exerting steric or hydrophilic effects on the heme configuration in the pocket. Indeed, the bandwidth of the iron-bound CO stretch is slightly different in diacetyldeutero-substituted PaTDO from those of other heme-substituted enzymes, probably indicating that the difference in the size, shape, or hydrophilicity of the acetyl side chains may affect the conformational freedom of the bound CO. The structural restriction in the distal side imposed by the acetyl side chains also caused slight resistance for the approach of O_2 to the heme, as shown by the small decrease of the O_2 association rate constant and by a large increase in O_2 equilibrium constants in comparison with that of proto- and meso-TDO (Figure 7 A,C). However, the steric and/or hydrophilic effect is not serious for other enzymatic properties, which are crucial for assessing the inductive electronic effect of the heme substituents. For instance, in the relationship of several properties of the heme-substituted PaTDO with pK_3 of the porphyrins, such as redox potentials (Figure 5), the νC−O positions (Figure 6), and the kinetic O_2 dissociation rate (Figure 7B), there is no significant deviation with respect to diacetyldeutero-PaTDO. These observations support the conclusion that the steric effect or hydrophilic property of the heme side chains on the key functional properties of PaTDO (i.e., redox potentials, νC−O, and k_{off} for O_2) can be practically eliminated, and that these altered enzymatic properties, stated above, mainly resulted from changes in the electron-withdrawing effects, rather than other effects of the heme substituents.

Mechanism of the Initial Step for TDO Dioxygenation Reaction. We demonstrated the linear relationships between several enzymatic properties of reconstituted PaTDO and the pK_3 of porphyrins. In these relationships, it is shown that diacetyldeutero-PaTDO has the most electron-deficient ferrous heme and exhibits the highest enzymatic activity among reconstituted PaTDOs.

Direct examination of the effects of the heme substituent on the reactivity of the ferrous−oxy complex should be required to elucidate the reaction mechanism of TDO. For instance, the H atom abstraction activity of compound III of HRP (formulated as $Fe^{2+}-O_2$ or $Fe^{3+}-O_2^-$) linearly decreased with an increase in the level of electron withdrawal of the heme substituents.[53] This reactivity trend revealed that an increase in the electron-withdrawing effects diminished the ability of the heme-bound O_2 to serve as an oxidant, probably by decreasing the π back-donation from the ferrous heme iron to the O_2 moiety.[54,55] This was an important clue in understanding the relation between the electronic state and the catalytic reactivity of the heme-bound O_2. However, such an experimental approach was impractical for PaTDO, because of the rapid autoxidation of the ferrous−oxy form in the absence of L-Trp. Nonetheless, in the case of PaTDO, it is reasonable to assume that the heme substituents modulate the reactivity of the ferrous−oxy heme by the π back-donation mechanism, as supported by the correlation between the electron withdrawal of the heme substituents and the dissociation rate of the bound O_2 (Figure 7). These results taken together lead to an important conclusion that the stronger electron-withdrawing heme substituents produce the more electron-deficient ferrous−oxy PaTDO. Hence, it is reasonable to propose that the electron-deficient ferrous−oxy heme is more reactive for the initial step of the catalytic dioxygenation by PaTDO. In other words, our results substantiate that the direct electrophilic addition of O_2 with the indole of L-Trp is the most likely pathway for the initial O_2 insertion reaction catalyzed by PaTDO (Scheme 1A,B).

TDO Mechanism Involves the Ferryl−Oxo Form or Not. One may note that the electron-deficient ferryl−oxo heme is less basic, as well. It has been generally accepted that the stronger electron-withdrawing axial ligand produces the more electron-deficient ferryl−oxo heme (i.e., less basic ferryl−oxo heme).[48] Recent studies of model heme complexes revealed that the enhanced electron-withdrawing ability of the axial ligand diminished the H atom abstraction activity of ferryl−oxo heme.[56] This reactivity trend is ascribed mainly to a decrease in the basicity of the ferryl−oxo heme.[56,57] The analogous relation has been observed for the inductive effects of the peripheral heme substituents on the H-abstraction activities of the ferryl−oxo heme of heme-substituted HRP.[26] The resonance Raman data that reveal that the hydrogen bond between the ferryl−oxo heme and the distal base was weaker in diacetyldeutero-HRP than proto-HRP[58] appear to support the basicity hypothesis. The formation of the ferryl−oxo heme in the TDO-catalyzed dioxygenation is underlined as a key intermediate in the heterolytic cleavage of the C_2-C_3 bond (Scheme 1B) or the ring opening of the Trp epoxide (Scheme 1C). In both pathways, the ferryl−oxo heme serves as a nucleophile in the

DOI: 10.1021/acs.biochem.5b00048
Biochemistry 2015, 54, 3604−3616

epoxide ring opening reaction,[21] and therefore, the more basic, electron-rich ferryl−oxo heme is favored to promote the reactions. This heme substitution study of PaTDO is likely not to support the possible involvement of the ferryl−oxo heme-dependent chemical step(s) in the mechanism. This is because the dioxygenase activity oppositely relates to the basic nature of the ferryl−oxo heme, as shown by the enhanced trend of the dioxygenase activity with an increase in the electron-withdrawing nature of the heme substituents.

Modulation of Reactivity of TDO by Trp Binding and Proximal His Ligand. It is noted that the midpoint potential of PaTDO is much higher than that of XcTDO in the absence of L-Trp: +82 mV for PaTDO versus +10 mV for XcTDO. This may come from the difference in the electron-donating nature of the proximal His. However, the difference in the redox potential was less relevant to their catalytic behaviors, because the L-Trp binding elevated the redox potential of both enzymes to 150−180 mV and led to virtually identical enzymatic activities. Likewise, L-Trp binding elevates the redox potential of rat liver TDO from −15 to 75 mV at pH 7.4 (data not shown). These values underline the role of L-Trp to serve as an effector. There is no reason to doubt that such a large increase in the redox potential in response to L-Trp binding is tuned by the relative binding affinity of L-Trp between the ferric enzyme and the ferrous enzyme and in turn stabilizes the ferrous heme iron by reducing the electron density of the heme iron.[15,52] The most straightforward way to rationalize the effects of L-Trp on the redox potential is to conclude that the binding of L-Trp promotes the formation of the electron-deficient ferrous−oxy heme to optimize the direct electrophilic addition of O_2. Recent observation of the linear correlation between the enzymatic activity of mutant IDOs and their midpoint potential[59] supports the hypothesis given above.

In conclusion, this heme-modification study provides the molecular basis for supporting the idea that the initial step of the O_2 insertion in the PaTDO-catalyzed dioxygenation is a direct electrophilic (two-electron transfer) addition of the heme-bound O_2 to the electron-rich indole carbon, rather than radical addition (one-electron transfer) pathway. This is also consistent with the recent mechanistic proposal from a mutational study of IDO and TDOs[17] and accounts for why 1-methyl-Trp is utilized as a substrate. However, our results do not rule out the possibility of the radical mechanism with respect to the IDO-catalyzed dioxygenation,[25] because the electron-donating anionic His residue is capable of producing the electron-rich ferrous−oxy and ferryl−oxo forms. Indeed, the Fe−His stretching frequency of human IDO (236 cm^{-1}) is significantly higher than that of PaTDO (216 cm^{-1}),[60] indicating that the proximal His of IDO is anionic imidazolate and has an electron-donating ability greater than that of neutral imidazole of PaTDO. Furthermore, the electron-donating effect of the His residue in IDO may be virtually unaffected upon L-Trp binding, as shown by a minor effect of L-Trp on the midpoint potential.[61] A definitive explanation for the difference in TDO- and IDO-catalyzed dioxygenase reactions requires further experiments.

■ ASSOCIATED CONTENT

Supporting Information

Optical absorption spectra of protoheme-reconstituted PaTDO (Figure S1), redox titration of meso- and deutero-PaTDO (Figure S2), stopped-flow traces of O_2 binding of meso-PaTDO (Figure S3), O_2 affinity measurements of meso-, proto-, and diacetyldeutero-PaTDO (Figure S4), and Michaelis−Menten kinetics for the K_m of O_2 (Figure S5). The Supporting Information is available free of charge on the ACS Publications website at DOI: 10.1021/acs.biochem.5b00048.

■ AUTHOR INFORMATION

Corresponding Authors

*Telephone: 81-042-747-0658. E-mail: rmakino04@rikkyo.ac.jp.

*Telephone: 81-0791-58-2817. E-mail: yshiro@riken.jp.

Funding

This work was supported by the Strategic Research Foundation Grant-aided Project for Private Universities (S12010039) from the Ministry of Culture, Education, Sports, Science and Technology of Japan.

Notes

The authors declare no competing financial interest.

■ ACKNOWLEDGMENTS

We thank Mieko Taketsugu for helpful technical assistance.

■ ABBREVIATIONS

TDO, L-tryptophan 2,3-dioxygenase; IDO, indoleamine 2,3-dioxygenase; NO, nitric oxide; CO, carbon monoxide; L-Trp, L-tryptophan; PaTDO, TDO from *Pseudomonas acidovorans*; XcTDO, TDO from *Xanthomonas campestris*; HRP, horseradish peroxidase; cytochrome P450cam, cytochrome P450 from *Pseudomonas putida*; KP_i, potassium phosphate; SDS−PAGE, sodium dodecyl sulfate−polyacrylamide gel electrophoresis; K_d, dissociation constant; k_{on}, association rate constant; k_{off}, dissociation rate constant; HPLC, high-performance liquid chromatography; EPR, electron paramagnetic resonance; k_{cat}, maximal turnover number of enzyme activity; E_m, midpoint potential.

■ REFERENCES

(1) Knox, W. E., and Mehler, A. H. (1950) The conversion of tryptophan to kynurenine in liver. I. The coupled tryptophan peroxidase-oxidase system forming formylkynurenine. *J. Biol. Chem. 187*, 419−430.

(2) Hayaishi, O., and Stanier, R. Y. (1951) The bacterial oxidation of tryptophan III: Enzymatic activities of cell-free extracts from bacteria employing the aromatic pathway. *J. Bacteriol. 62*, 691−709.

(3) Tanaka, T., and Knox, W. E. (1959) The nature and mechanism of the tryptophan pyrrolase (peroxidase-oxidase) reaction of *Pseudomonas* and of rat liver. *J. Biol. Chem. 234*, 1162−1170.

(4) Greengard, O., and Feigelson, P. (1962) The purification and properties of liver tryptophan pyrrolase. *J. Biol. Chem. 237*, 1903−1907.

(5) Hayaishi, O., Rothberg, S., Mehler, A. H., and Saito, Y. (1957) Studies on oxygenases. Enzymatic formation of kynurenine from tryptophan. *J. Biol. Chem. 229*, 889−896.

(6) Yamamoto, S., and Hayaishi, O. (1967) Tryptophan pyrrolase of rabbit intestine. D- and L-Tryptophan-cleaving enzyme or enzymes. *J. Biol. Chem. 242*, 5260−5266.

(7) Hayaishi, O. (1976) Properties and function of indoleamine 2,3-dioxygenase. *J. Biochem. 79*, 13−21.

(8) Ishimura, Y., Nozaki, M., Hayaishi, O., Tamura, M., and Yamazaki, I. (1967) Evidence for an oxygenated intermediate in the tryptophan pyrrolase reaction. *J. Biol. Chem. 242*, 2574−2576.

(9) Ishimura, Y., Nozaki, M., Hayaishi, O., Nakamura, T., Tamura, M., and Yamazaki, I. (1970) The oxygenated form of L-tryptophan 2,3-dioxygenase as reaction intermediate. *J. Biol. Chem. 245*, 3593−3602.

(10) Sugimoto, H., Oda, S., Otsuki, T., Hino, T., Yoshida, T., and Shiro, Y. (2006) Crystal structure of human indoleamine 2,3-

DOI: 10.1021/acs.biochem.5b00048
Biochemistry 2015, 54, 3604−3616

dioxygenase: Catalytic mechanism of O_2 incorporation by a heme-containing dioxygenase. *Proc. Natl. Acad. Sci. U.S.A. 103*, 2611−2616.
(11) Forouhar, F., Anderson, J. L., Mowat, C. G., Vorobiev, S. M., Hussain, A., Abashidze, M., Bruckmann, C., Thackray, S. J., Seetharaman, J., Tucker, T., Xiao, R., Ma, L.-C., Zhao, L., Acton, T. B., Montelione, G. T., Chapman, S. K., and Tong, L. (2007) Molecular insights into substrate recognition and catalysis by tryptophan 2,3-dioxygenase. *Proc. Natl. Acad. Sci. U.S.A. 104*, 473−478.
(12) Zhang, Y., Kang, S. A., Mukherjee, T., Bale, S., Crane, B. R., Begley, T. P., and Ealick, S. E. (2007) Crystal structure and mechanism of tryptophan 2,3-dioxygenase, a heme enzyme involved in tryptophan catabolism and in quinolinate biosynthesis. *Biochemistry 46*, 145−155.
(13) Hamilton, G. A. (1969) Mechanisms of two- and four-electron oxidations catalyzed by some metalloenzymes. *Adv. Enzymol. Relat. Areas Mol. Biol. 32*, 55−96.
(14) Sono, M., Roach, M. P., Coulter, E. D., and Dawson, J. H. (1996) Heme-containing oxygenases. *Chem. Rev. 96*, 2841−2888.
(15) Thackray, S. J., Bruckmann, C., Anderson, J. L. R., Campbell, L. P., Xiao, R., Zhao, L., Mowat, C. G., Forouhar, F., Tong, L., and Chapman, S. K. (2008) Histidine 55 of tryptophan 2,3-dioxygenase is not an active site base but regulates catalysis by controlling substrate binding. *Biochemistry 47*, 10677−10684.
(16) Batabyal, D., and Yeh, S.-R. (2009) Substrate-protein interaction in human tryptophan dioxygenase: The critical role of H76. *J. Am. Chem. Soc. 131*, 3260−3270.
(17) Chauhan, N., Thackray, S. J., Rafice, S. A., Eaton, G., Lee, M., Efimov, I., Bastran, J., Jenkins, P. R., Mowat, C. G., Chapman, S. K., and Raven, E. L. (2009) Reassessment of the reaction mechanism in the heme dioxygenase. *J. Am. Chem. Soc. 131*, 4186−4187.
(18) Geng, J., Darnevil, K., and Liu, A. (2012) Chemical rescue of the distal histidine mutants of tryptophan 2,3-dioxygenase. *J. Am. Chem. Soc. 134*, 12209−12218.
(19) Chung, L. W., Li, X., Sugimoto, H., Shiro, Y., and Morokuma, K. (2008) Density functional theory study on a missing piece in understanding of heme chemistry: The reaction mechanism for indoleamine 2,3-dioxygenase and tryptophan 2,3-dioxygenase. *J. Am. Chem. Soc. 130*, 12299−12309.
(20) Capece, L., Lewis-Ballester, A., Batabyal, D., Russo, N. D., Yeh, S.-R., Estrin, D. A., and Marti, M. A. (2010) The first step of the dioxygenation reaction carried out by tryptophan dioxygenase and indoleamine 2,3-dioxygenase as revealed by quantum mechanical/molecular mechanical studies. *JBIC, J. Biol. Inorg. Chem. 15*, 811−823.
(21) Basran, J., Efimov, I., Chauhan, N., Thackray, S. J., Krupa, J. L., Eaton, G., Griffith, G. A., Mowat, C. G., Handa, S., and Raven, E. L. (2011) The mechanism of formation of N-formylkynurenine by heme dioxygenase. *J. Am. Chem. Soc. 133*, 16251−16257.
(22) Chung, L. W., Li, X., Sugimoto, H., Shiro, Y., and Morokuma, K. (2010) ONIOM study on a missing piece in our understanding of heme chemistry: Bacterial tryptophan 2,3-dioxygenase with dual oxidants. *J. Am. Chem. Soc. 132*, 11933−12005.
(23) Capece, L., Lewis-Ballester, A., Yeh, S.-R., Estrin, D. A., and Marti, M. A. (2012) Complete reaction mechanism of indoleamine 2,3-dioxygenase as revealed by QM/MM simulations. *J. Phys. Chem. B 116*, 1401−1413.
(24) Efimov, I., Bastran, J., Thacray, S. J., Handa, S., Mowat, C. G., and Raven, E. L. (2011) Structure and reaction mechanism in the heme dioxygenases. *Biochemistry 50*, 2717−2724.
(25) Lewis-Ballester, A., Batabyal, D., Egawa, T., Lu, C., Lin, Y., Marti, M. A., Capese, L., Estrin, D. A., and Yeh, S.-R. (2009) Evidence of a ferryl intermediate in a heme-based dioxygenase. *Proc. Natl. Acad. Sci. U.S.A. 106*, 17371−17376.
(26) Makino, R., and Yamazaki, I. (1972) Effects of 2,4-substituents of deuterohemin upon peroxidase functions: 1. Preparation and some properties of artificial enzymes. *J. Biochem. 72*, 655−664.
(27) Makino, R., and Yamazaki, I. (1974) Effects of 2,4-substituents of deuteroheme upon peroxidase functions. Reactions of peroxidase and myoglobin with oxygen, carbon monoxide and alkylisocyanides. *Arch. Biochem. Biophys. 165*, 485−493.
(28) Sono, M., and Asakura, T. (1975) Decrease in oxygen affinity of myoglobin by formylation of vinyl groups of heme. *J. Biol. Chem. 250*, 5227−5232.
(29) Seybert, D. W., Moffat, K., Gibson, Q. H., and Chang, C. K. (1977) Electronic and steric factors affecting ligand binding: Horse hemoglobins containing 2,4-dimethyldeuteroheme and 2,4-dibromo-deuteroheme. *J. Biol. Chem. 252*, 4225−4231.
(30) Yamada, H., Makino, R., and Yamazaki, I. (1975) Effects of 2,4-substituents of deuteroheme upon redox potentials of horseradish peroxidases. *Arch. Biochem. Biophys. 169*, 344−353.
(31) Makino, R., Iizuka, T., Sakaguchi, K., and Ishimura, Y. (1983) Effects of heme substitution on the activity of heme-containing oxygenases. In *Oxygenases and oxygen metabolism (A symposium in honor of Osamu Hayaishi)*, pp 467−477, Academic Press, New York.
(32) Falk, J. E. (1964) *Porphyrins and metallporphyrins*, pp 115−180. Elsevier Publishing Co., Amsterdam.
(33) Caughey, W. S., Alben, J. O., Fujimoto, W. Y., and York, J. L. (1966) Substituted deuteroporphyrins. I. Reactions at the periphery of the porphyrin ring. *J. Org. Chem. 31*, 2631−2640.
(34) Makino, R., Sakaguchi, K., Iizuka, T., and Ishimura, Y. (1980) Acid-alkaline transition and thermal spin equilibrium of the heme in ferric L-tryptophan 2,3-dioxygenases. *J. Biol. Chem. 255*, 11883−11891.
(35) Poillon, W. N., Maeno, H., Koike, K., and Feigelson, P. (1969) Tryptophan oxygenase of *Pseudomonas acidovorans*. Purification, composition and subunit structure. *J. Biol. Chem. 244*, 3447−3456.
(36) Yu, C. A., and Gunsalus, I. C. (1974) Cytochrome $P\text{-}450_{cam}$. III. Removal and replacement of ferriprotoporphyrin IX. *J. Biol. Chem. 249*, 107−110.
(37) Chance, B. (1947) The kinetics of the enzyme-substrate compound of peroxidase. *J. Biol. Chem. 151*, 553−577.
(38) Yonetani, T. (1961) Studies on Cytochrome Oxidase. III. Improved Preparation and Some Properties. *J. Biol. Chem. 236*, 1680−1688.
(39) Ishimura, Y., Makino, R., Ueno, R., Sakaguchi, K., Brady, F. O., Feigelson, P., Aisen, P., and Hayaishi, O. (1980) Copper is not essential for the catalytic activity of L-tryptophan 2,3-dioxygenase. *J. Biol. Chem. 255*, 3835−3837.
(40) Brady, F. O., Monaco, M. E., Forman, H. J., and Feigelson, P. (1972) On the Role of Copper in Activation of and Catalysis by Tryptophan-2,3-dioxygenase. *J. Biol. Chem. 247*, 7915−7922.
(41) Ishimura, Y., and Hayaishi, O. (1973) Noninvolvement of Copper in the L-Tryptophan 2,3-Dioxygenase Reaction. *J. Biol. Chem. 248*, 8610−8612.
(42) Yonetani, T., Yamamoto, H., Erman, J. E., Leigh, J. S., and Reed, G. H. (1972) Electromagnetic properties of hemoproteins. V. Optical and electron paramagnetic resonance characteristics of nitric oxide derivatives of metalloporphyrin-apohemoprotein complexes. *J. Biol. Chem. 247*, 2447−2455.
(43) Henry, Y., Ishimura, Y., and Peisach, J. (1976) Binding of nitric oxide to reduced L-tryptophan 2,3-dioxygenase as studied by electron paramagnetic resonance. *J. Biol. Chem. 251*, 1578−1581.
(44) Falk, J. E. (1964) *Porphyrins and metallporphyrins*, pp 28, Elsevier Publishing Co., Amsterdam.
(45) Uchida, K., Bandow, H., Makino, R., Sakaguchi, K., Iizuka, T., and Ishimura, Y. (1985) Infrared spectra of carbon monoxide complexes of indoleamine 2,3-dioxygenase and L-tryptophan 2,3-dioxygenases. *J. Biol. Chem. 260*, 1400−1406.
(46) Batabyal, D., and Yeh, S.-R. (2007) Human tryptophan dioxygenase: A comparison to indoleamine 2,3-dioxygenase. *J. Am. Chem. Soc. 129*, 15690−15701.
(47) Schlichting, I., Berendzen, J., Chu, K., Stock, A. M., Maves, S. A., Benson, D. E., Sweet, R. M., Ringe, D., Petsko, G. A., and Sligar, S. G. (2000) The catalytic pathway of cytochrome P450cam at atomic resolution. *Science 284*, 1615−1622.
(48) Oberting, W. A., Kean, R. T., Wever, R., and Babcock, G. T. (1990) Factors affecting the iron-oxygen vibrations of ferrous oxy and ferryl oxo heme proteins and model compounds. *Inorg. Chem. 29*, 2633−2645.

DOI: 10.1021/acs.biochem.5b00048
Biochemistry 2015, 54, 3604−3616

(49) Capece, L., Marti, M. A., Crespo, A., Doctorovich, F., and Estrin, D. A. (2006) Heme protein oxygen affinity regulation exerted by proximal effects. *J. Am. Chem. Soc. 128*, 12455−12461.
(50) Marti, M. A., Crespo, A., Capece, L., Boechi, L., Bikiel, D. E., Scherlis, D. A., and Estrin, D. A. (2006) Dioxygen affinity in heme proteins investigated by computer simulation. *J. Inorg. Biochem. 100*, 761−770.
(51) Tsai, A.-l., Martin, E., Berka, V., and Olson, J. S. (2012) How do heme-protein sensors exclude oxygen? Lessons learned from cytochrome c′, *Nostoc putiforme* heme nitric oxide/oxygen-binding domain, and soluble guanylate cyclase. *Antioxid. Redox Signaling 17*, 1246−1262.
(52) Basran, J., Rafice, S. A., Chauhan, N., Efimov, I., Chessman, M. R., Ghamsari, L., and Raven, E. L. (2008) A kinetic, spectroscopic, and redox study of human tryptophan 2,3-dioxygenase. *Biochemistry 47*, 4752−4760.
(53) Makino, R., Yamada, H., and Yamazaki, I. (1976) Effects of 2,4-substituents of deuteroheme upon the stability of the oxy-form and compound I of horseradish peroxidases. *Arch. Biochem. Biophys. 173*, 66−70.
(54) Bikiel, D. E., Bari, S. E., Dotorovich, F., and Estrin, D. A. (2008) DFT study on the reactivity of iron porphyrins tuned by ring substitution. *J. Inorg. Chem. 102*, 70−76.
(55) Lai, W., and Shaik, S. (2011) Can ferric-superoxide acts as a potential oxidant in P450cam? QM/MM investigation of hydroxylation, epoxidation, and sulfoxidation. *J. Am. Chem. Soc. 133*, 5444−5452.
(56) Kang, Y., Chen, H., Jeong, Y. J., Lai, W., Bae, E. H., Shaik, S., and Nam, W. (2009) Enhanced reactivities of iron(IV)-oxo porphyrin π-cation radicals in oxygenation reactions by electron-donating axial ligands. *Chem.—Eur. J. 15*, 10039−10046.
(57) Green, M. T., Dawson, J. H., and Gray, H. B. (2004) Oxoiron(IV) in chloroperoxidase compound II is basic: Implications for P450 chemistry. *Science 304*, 1653−1656.
(58) Makino, R., Uno, T., Nishimura, Y., Iizuka, T., Tsuboi, M., and Ishimura, Y. (1986) Coordination structures and reactivities of compound II in iron and manganese horseradish peroxidases. A resonance Raman study. *J. Biol. Chem. 261*, 8376−8382.
(59) Efimov, I., Basran, J., Sun, X., Chauhan, N., Chapman, S. K., Mowat, C. G., and Raven, E. L. (2012) The mechanism of substrate inhibition in human indoleamine 2,3-dioxygenase. *J. Am. Chem. Soc. 134*, 3034−3041.
(60) Terentis, A. C., Thomas, S. R., Takikawa, O., Littlejohn, T. K., Truscott, R. J. W., Armstrong, R. S., Yeh, S.-R., and Stocker, R. (2002) The heme environment of recombinant human indoleamine 2,3-dioxygenase. *J. Biol. Chem. 277*, 15788−15794.
(61) Papadopoulou, N. D., Mewies, M., McLean, K. J., Seward, H. E., Svistunenko, D. A., Munro, A. W., and Raven, E. L. (2005) Redox and spectroscopic properties of human indoleamine 2,3-dioxygenase and a His303Ala variant: Implications for catalysis. *Biochemistry 44*, 14318−14328.

DOI: 10.1021/acs.biochem.5b00048
Biochemistry 2015, 54, 3604−3616